Energy Management for an AC Island Microgrid Using Dynamic Programming

Wassim Chouaf*‡, Ahmed Abbou*, Abdessamade Bouaddi*

*Department of Electrical Engineering, Mohammadia School of Engineers (EMI), Mohammed V University, Rabat, Morocco
(wassim.chouaf.emi@gmail.com, abbou@emi.ac.ma, bouaddi47@gmail.com)

‡Corresponding Author; Wassim Chouaf, Bernoussi Casablanca, Tel: +212664314301, wassim.chouaf.emi@gmail.com

Received: 23.10.2022 Accepted: 28.11.2022

Abstract- This paper presents an optimal Energy Management Strategy for distributed generations in AC island microgrid. The considered microgrid consists of PV generator, wind turbine, gas turbine, battery, supercapacitor, load, electric vehicle and hydrogen energy storage system consisting of fuel cell, electrolyzer and hydrogen tank. A centralized control has been used in this work to optimize the energy management while ensuring a power balance between production and consumption as well as optimal operating conditions. Two predictive energy control strategies, i.e. requiring predictive data, based on dynamic programming and rule-based strategy have been proposed for this topology. The main goal is to minimize the operating cost of the system and to maintain the balance between generation and consumption as well as optimal operating conditions. Indeed, some input data are difficult to predict with a good reliability. To cope with these prediction errors, so-called "reactive" algorithms are developed, capable of modifying the predictive strategy according to the prediction errors and aiming at predetermining the production profile of the generators, in order to achieve a comprehensive optimization of an objective function for the power system and subsequently adjust the operating points during the day. Simulations are performed to test the performance of the methods proposed.

Keywords Energy Management System; Battery Energy Storage System; Dynamic programming; Hybrid Energy System, Renewable Energy Sources; Distributed Energy Resources.

Nomenclature

$P_{elec}(t)$: Power of the electrolyzer at time t.
$P_{gt}(t)$: Power delivered by the gas turbine at time t.
$P_{wt}(t)$: Power delivered by the wind turbine at time t.
$P_{pv}(t)$: Power delivered by the photovoltaic panels at time t.
$P_{sc}(t)$: Supercapacitor power at time t.
$P_{fc}(t)$: Fuel cell power at time t.
$P_{bcar}(t)$: Electric car battery power at time t.
$P_{load}(t)$: Load power at time t.
$P_{batt}^{min}, P_{batt}^{max}$: Minimum and maximum power of the BESS.
$P_{bcar}^{min}, P_{bcar}^{max}$: Minimum and maximum power of the car battery.
$P_{gt}^{min}, P_{gt}^{max}$: Minimum and maximum power of the gas turbine.
$P_{gt,nom}$: Nominal power of the gas turbine.
$Q_{H2}(t)$: Energy equivalent of stored hydrogen at time t.
Q_{H2max}: Capacity of the hydrogen tank.
$C_{batt}(t)$: Storage capacity of the BESS system at time t.
C_{batt}^{ref}: Reference storage capacity of the BESS system.
C_{bcar}^{ref}: Reference storage capacity of the car battery.
$SOC_{batt}(t)$: State of charge of the BESS system at time t.
$SOC_{bcar}(t)$: State of charge of the car battery at time t.
$\Delta SOC_{batt}(t)$: Variation of the state of charge of the BESS system at time t.
$\Delta SOC_{bcar}(t)$: Variation of the state of charge of the car battery at time t.
$SOC_{batt}^{min}, SOC_{batt}^{max}$: SOC minimum and maximum value of the BESS.
$SOC_{bcar}^{min}, SOC_{bcar}^{max}$: SOC minimum and maximum value of the car battery.
Δt: Time step.
$\Delta SOC_{batt}^{min}, \Delta SOC_{batt}^{max}$: Minimum and maximum variation of the state of charge of the BESS.
$\Delta SOC_{bcar}^{min}, \Delta SOC_{bcar}^{max}$: Minimum and maximum variation of the state of charge of the car battery.
$SOH_{batt}(t)$: BESS State of health at time t.
$SOH_{bcar}(t)$: Car battery state of health at time t.
SOH_{min} : Minimum State of health of the storage systems.

NH(t) : Hydrogen storage level in the tank at time t.
NH_{min} : Minimum level of hydrogen storage.
BrC : Battery replacing cost ($).
CH : Cost of using the hydrogen system ($).
CG : Cost of using the gas turbine ($).
$C_{gt,Pen}$: Cost penalty per kWh generated by the gas turbine.
N_{pv} : Number of PV modules.
G^R : Reference of solar irradiation [W/m²].
$\eta_{p,max}$: Power variation with temperature [W /°C].
NOCT : Normal operating temperature of the cell [C].
T_j^R : Module temperature at standard conditions [°C].

1. Introduction

The increase in global energy demand and the pursuit of sustainable development have led to the increasing integration of renewable energy sources into the grid. However, the production of renewable energy sources is intermittent, which poses a serious challenge for small capacity microgrids [1]. Microgrids are now recognized as a key factor in the transition to smarter and cleaner energy systems, but due to the intermittency of renewable sources, which depends on uncontrollable conditions, for example solar irradiation and wind speed, an energy management system is necessary, especially when there are multiple resources, in order to find the best power distribution between the different elements that compose the hybrid energy system (HES), to improve the stability of the microgrid system, to ensure despite the strong variations of the produced energy, the electrical energy need of the load, to supply the load demand at any time, to reduce the use of storage elements to the minimum, to extend the life of the HES and to minimize the cash flow of the system.

The system analysed in this study uses wind and photovoltaic generation as a distributed renewable resource, lithium-ion batteries as a short-term energy storage element, a supercapacitor, to reduce battery stress, eliminate peak current, and minimize power fluctuations, hydrogen fuel cells as a long-term storage element, and a gas turbine as a secondary source. Daily forecasts of photovoltaic and wind generation and electrical load are used in an optimization algorithm to determine the charging/discharging schedule of the storage system during the day taking into account the intermittency of renewable sources. Therefore, an energy management system (EMS) is needed when there are different resources.

Optimal energy management of microgrids has been addressed in several recent literatures. For example, fuzzy logic-based EMS was presented in [1, 2, 3]. In [4, 5], optimal energy management, for a connected grid with a PV, battery and vehicle power system, is addressed using quadratic programming (QP). The particle swarm optimization (PSO) technique is proposed in [6, 7, 8]. In [9], A machine learning algorithm was used to solve the EMS. The operation and control of a DC microgrid in grid-connected and isolated modes is explained in [10]. An energy management of hybrid microgrid with hybrid energy storage system has been proposed in [11,12]. An energy management in the decentralized generation systems based on renewable energy sources was presented in [13]. An optimal energy management using a two-stage rolling horizon technique for Controlling an energy storage system was presented in [14]. Dynamic programming (DP) and advanced dynamic programming (ADP) are used to optimize energy management in [15]. A genetic algorithm optimization module is used to search for the optimal production schedule in [16, 17]. A dynamic energy management algorithm (DEM) has been proposed in [18]. A mixed integer linear programming (MILP) based strategy is used to find the optimal energy management in [19, 20]. A performance enhancement of hybrid solar PV-Wind system based on fuzzy power management strategy was presented in [21]. A photovoltaic, wind, and single-phase AC battery-based search of the energy management strategy and the cost of optimizing the system operation and battery life has been proposed in the literature [22]. A rule-based EMS management has been proposed in [23].

In this work, two energy management strategies have been proposed to optimize the performance of power systems including both variables generation and energy storage components. The first one is a rule-based management that guarantees compliance with the imposed constraints but has some limitations that we will expose. The second one is a predictive management strategy based on dynamic programming, from the considered known predictive data, which uses the Bellman-Ford algorithm to determine the shortest path through a network and performs a thorough analysis of the system performance and incorporates a battery health check in the decision-making process. To cope with the prediction errors and to be able to adapt the two developed strategies according to the prediction errors, correction algorithms have been developed to improve the stability of the microgrid system with optimal management by ensuring a power balance between production and consumption and to have the best energy and economic performance. The two methods will be compared primarily in terms of economic performance criteria.

In this paper, the configuration of the microgrid is described in Section 2. The methodology is shown in Section 3. Dynamic programming method is described in Section 4. Rule-based method is presented in Section 5. Results and discussion are shown in Section 6. Energy Management Strategies with correction are described in Section 7. The paper is concluded in the last Section.

2. Microgrid Configuration

A hybrid system comprising a photovoltaic generator, a wind turbine, a gas turbine, a battery (BESS), a supercapacitor, a load, an electric vehicle, and a hydrogen energy storage system consisting of a fuel cell, an electrolyzer, and a hydrogen tank is shown in Fig.1:

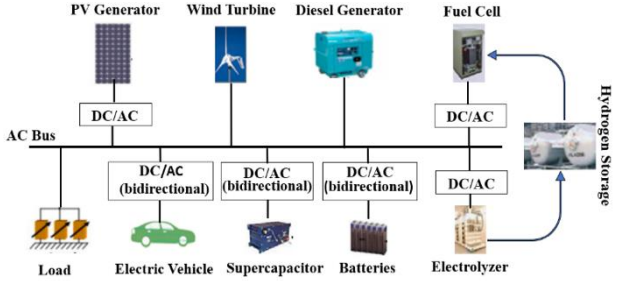

Fig. 1. The configuration of the studied microgrid.

2.1 Photovoltaic System

The calculation of the photov oltaic power produced is based on a simplified model of solar panels. An electrical circuit equivalent to a diode of photovoltaic cells and which mainly takes into account the solar irradiation Gin (in W/m²), the ambient temperature T (in °C) and the different characteristics of the panels considered, as represented in equation (1) [24]:

$$P_{pv}(G_{in}, T) = N_{pv}\frac{G_{in}}{G^R}(P_{pv,max} + \eta_{p,max}\left(T + G_{in}\frac{NOCT - 20}{800} - T_j^R\right)) \quad (1)$$

The efficiency of the DC/AC converter is assumed to be equal to 1. The PV production curve is shown in Fig.2:

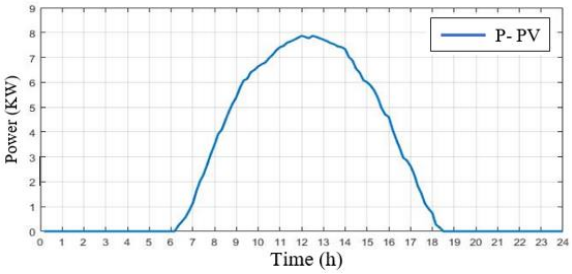

Fig. 2. The hourly data of PV system production.

2.2 Wind Turbine Model

The wind energy is calculated by (2).

$$E_k = \frac{1}{2} \times m \times v^2 \quad (2)$$

The power supplied by the turbine rotor from the wind will be derived from (3).

$$P_{wt} = \frac{1}{2} \times k_m \times (v^2 - v_0^2) \quad (3)$$

Where:

v: wind speed before turbine.
v_o: wind speed after turbine.

$$k_m = \rho \times A \times \frac{v + v_0}{2} \quad (4)$$

Finally, the power of the turbine will be calculated by (5) [25, 26]:

$$P_{wt} = \frac{1}{2} \times \rho \times A \times v^3 \times C_p \quad (5)$$

Where " Cp " is the rotor coefficient.

Figure 3 shows the wind power profile generated for 24H.

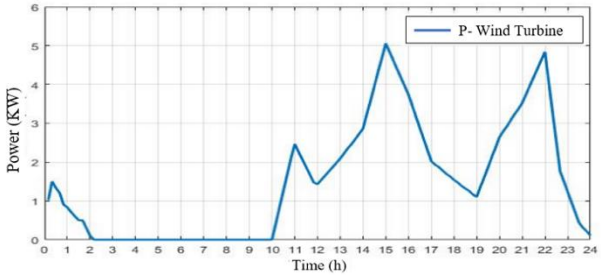

Fig. 3. The hourly data of wind turbine production.

2.3 Battery Energy Storage System (BESS)

The batteries are discharged only when there is insufficient generation from renewable sources, depending on the battery's state of charge (SOC), and are recharged as soon as possible, only from photovoltaic and wind sources, when there is an overproduction [15].

The state of charge (SOC) can be calculated using the equation (6):

$$SOC(t) = \frac{C_{batt}(t)}{C_{batt}^{ref}} \quad (6)$$

The state of charge of the batteries, at time t, is related to the state of charge at time t-1 and to the difference between the power produced (the one generated by the wind turbine and the photovoltaic production) and the power requested by the load, the calculation of the state of charge at time t can be expressed by the following equation (7):

$$SOC(t) = SOC(t-1)\frac{P_{PV}(t) + P_{wt}(t) - P_{load}(t)}{C_{batt}^{ref}} \times \Delta t \quad (7)$$

2.4 Hydrogen Energy Storage System (HESS)

The hydrogen storage system is composed of a hydrogen storage tank, an electrolyzer and a fuel cell. When there is an excess of energy (overproduction) and the batteries are fully charged, this surplus energy is used to produce hydrogen by electrolysis of water, which is then stored in the tank to be used by the fuel cell during periods when there is a lack of energy, in order to meet the load demand. The storage of hydrogen energy is limited by the storage capacity of the tank which is used within the minimum and maximum hydrogen storage limits. The energy of the hydrogen stored in the tank is given by the following equation (8) [28]:

$$Q_{H2}(t) = Q_{H2}(t_0) + \int (P_{elec} - P_{fc}).dt \quad (8)$$

To adapt this formula to our discrete model, it must be discretized as given below, equation (9):

$$Q_{H2}(k) = Q_{H2}(0) + \sum_{i=1}^{k} (P_{elec}(i) - P_{fc}(i)).\Delta t \quad (9)$$

The level of hydrogen storage in the tank (NH) is given in percentage as indicated in the following equation (10):

$$NH(i) = 100 \times \frac{Q_{H2}(i)}{Q_{H2max}} \quad (10)$$

2.5 Load

The load data used in this paper is based on the daily load curve of a household of 9 persons, as shown in Fig.4:

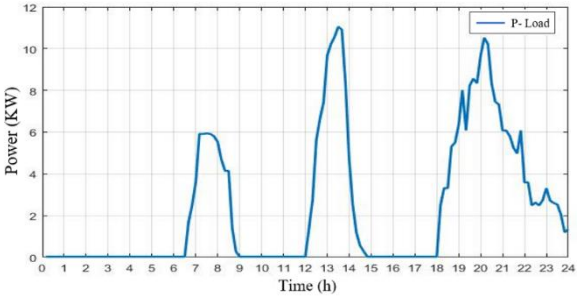

Fig. 4. The daily load curve.

The maximum daily power requested by the loads is 11.2 kW.

2.6 Supercapacitor Model

Supercapacitors are characterized by their instantaneous response time. In our case, they are used and sized to be able to substitute an excess of energy (overproduction) or a lack of energy (underproduction) for a period of 10 seconds, for each time step (Δt), and provided that this lack or excess of energy is greater than a minimum power of 0.5 kW.

2.7 Gas Turbine

The gas turbine consists of a permanent magnet synchronous machine providing AC power and a power conditioning system. It is used to cover the energy needed in case of insufficient energy supplied by the PV generator, wind turbine, battery and hydrogen storage system. It is preferable that the gas turbine not be used to generate less than 50% and more than 90% of its rated power ($P_{gt,nom}$) for performance reasons [27]. As given by the following equation (11):

$$0.5 \times P_{gt,nom} \leq P_{gt}(t) \leq 0.9 \times P_{gt,nom} \quad (11)$$

We used a simple and approximate first order linear model of a micro gas turbine with a response time of 10s ($\tau_{gt} = 10\ s$):

$$P_{gt}(t) = \frac{1}{1 + \frac{\tau_{gt}}{3}} \times P_{gt,nom} \quad (12)$$

This model is used to model the electrical power generated and the resulting calculations, assuming that the micro turbine is started.

2.8 Electric Vehicle

The electric car battery is considered a secondary storage system that can be used to ensure the power balance between load consumption and renewable sources generation and to minimize the cash flow of the system. In case of overproduction, if the BESS is fully charged and the hydrogen tank is filled to its maximum level, we can charge the electric car battery with this excess energy (within the limits imposed by the state of charge of the car battery). In case of underproduction and the BESS is completely discharged as well as the hydrogen tank is at its low level and to avoid starting the gas turbine, the battery of the electric car is used to cover this lack of energy. In both cases, the battery of the electric car can only be used in the periods when it is connected to the microgrid. In our case, the car is connected to the microgrid from 00h00 to 8h00 and from 5h00 to midnight.

3. Methodology

The optimization model of the microgrid energy management system is studied over 24 hours with a step size of 10 minutes. The decisive variables are photovoltaic power generation "P_{pv}", wind turbine power generation "P_{wt}", load demand "P_{load}", BESS power "P_{batt}", gas turbine power "P_{gt}", supercapacitor power "P_{sc}", electrolyzer power "P_{elec}", fuel cell power "P_{fc}" and electric car battery power "P_{bcar}". An appropriate switching control must optimize the total operating cost of the microgrid to satisfy all the equal and unequal energy transfer constraints.

The wind turbine, the photovoltaic generator, the gas turbine and the fuel cell are considered in generator mode. For the electrolyzer, the BESS, the electric car battery, the supercapacitor and the electrolyzer are in receiver convention.

3.1 Objective Function of the Cost Minimization

The objective function is to optimize the use of the battery energy storage system, the fuel cells and the gas turbine. The objective function is defined as follows:

$$min\big(CF(t)\big) = min \sum_{0}^{T} \big(BrC(t) + CG(t) + CH(t)\big) \quad (13)$$

The performance index is the sum of the cash flows CF which is defined as the difference between cash inflows and cash outflows generated by the activity (in this case energy production or consumption).

The battery replacement cost at each time step is the cost of replacing the capacity lost during the time interval Δt. The health state "SOH_{batt}^{min}" is defined as the state at which the user considers that the batteries should be replaced. The change in health state during the time interval is defined by equations (14) and (15). The cost of replacing the batteries at each time interval is calculated using equation (16). The "BiC" (Batteries investment Cost) is defined by equation (17):

$$\Delta SOH_{batt}(x_i, x_j, t) = SOH_{batt,x_i}(t - \Delta t) - SOH_{batt,x_j}(t) \quad (14)$$

$$\Delta SOH_{batt}(x_i, x_j, t) = Z.[SOC_{batt,x_j}(t + \Delta t - SOC_{batt,x_i}(t)] \quad (15)$$

$$\sum_{t,SOH=1}^{t,SOH=SOH_{batt}^{min}} BrC(t) = BiC \quad (16)$$

$$BrC(x_i, x_j, t) = BiC \times \left[\frac{\Delta SOH_{batt}(x_i, x_j, t)}{1 - SOH_{batt}^{min}}\right] \quad (17)$$

Where :

- Z is the Battery aging coefficient.
- xi is the state at time t and xj is the state at time t+Δt.

The cost of using the hydrogen system is represented by the following equations (18):

$$CH(t) = C_{fc} \times (a_{fc} \times P_{fc} + b_{fc}) \times \Delta t \quad (18)$$

With:

- afc, bfc are the cost parameters of the fuel cell use and Cfc the cost per kWh produced by the fuel cell.
- bfc is considered negligible (=0) and afc is assumed to be equal to 1.

A quadratic function is used to represent the cost of using the gas turbine:

$$CG(t) = C_{gt} \times (a_{gt} \times P_{gt}^2 + b_{gt} \times P_{gt} + c_{gt}) \times \Delta t \quad (19)$$

With:

- a_{gt}, bgt and c_{gt} are the cost parameters of the use of the gas turbine and C_{gt} is the cost per kWh generated by the gas turbine.
- a_{gt} and cgt considered negligible, bgt is assumed equal to 1.

3.2 Constraints

Balance constraint: Constraint (20) defines the power flow in the system following the physical principle of power conservation. This constraint stipulates that the power demanded by the load at any time of the day "P_{load}" must be equal to the sum of the photovoltaic energy production "P_{pv}", the wind energy production "P_{wt}", the power of the battery "P_{batt}", the power of the gas turbine "P_{gt}", the power of the supercapacitor "P_{sc}", the power of the electrolyzer "P_{elec}", the power of the fuel cell "P_{fc}", and the power of the electric car battery "P_{bcar}" [27, 29]:

$$P_{load} + P_{pv} + P_{wt} + P_{gt} + P_{fc} + P_{elec} + P_{batt} + P_{bcar} + P_{sc} = 0 \quad (20)$$

The equality and inequality constraints of the power distribution problem are expressed by the following equations:

$$SOC_{batt}^{min} \leq SOC_{batt}(t) \leq SOC_{batt}^{max} \quad (21)$$

$$SOC_{bcar}^{min} \leq SOC_{bcar}(t) \leq SOC_{bcar}^{max} \quad (22)$$

$$P_{batt}^{min} \leq |P_{batt}(t)| \leq P_{batt}^{max} \quad (23)$$

$$P_{bcar}^{min} \leq |P_{bcar}(t)| \leq P_{bcar}^{max} \quad (24)$$

$$\Delta SOC_{batt}^{min} \leq \Delta SOC_{batt} \leq \Delta SOC_{batt}^{max} \quad (25)$$

$$\Delta \mathrm{SOC}_{\mathrm{bcar}}^{\min} \leq \Delta \mathrm{SOC}_{\mathrm{bcar}}(t) \leq \Delta \mathrm{SOC}_{\mathrm{bcar}}^{\max} \quad (26)$$

$$\mathrm{SOH}_{\mathrm{batt}}(t) \geq \mathrm{SOH}_{\min} \quad (27)$$

$$\mathrm{SOH}_{\mathrm{bcar}}(t) \geq \mathrm{SOH}_{\min} \quad (28)$$

$$\mathrm{NH}_{\min} \leq \mathrm{NH}(t) \leq \mathrm{NH}_{\max} \quad (29)$$

$$\mathrm{P}_{\mathrm{gt}}^{\min} \leq \mathrm{P}_{\mathrm{gt}}(t) \leq \mathrm{P}_{\mathrm{gt}}^{\max} \quad (30)$$

$$\mathrm{P}_{\mathrm{sc}}^{\min} \leq |\mathrm{P}_{\mathrm{sc}}(t)| \quad (31)$$

Where:

$$\mathrm{P}_{\mathrm{batt}}(t) = ((\mathrm{SOC}_{\mathrm{batt}}(t + \Delta t) - \mathrm{SOC}_{\mathrm{batt}}(t)).\mathrm{V}_{\mathrm{dc}}.\mathrm{C}_{\mathrm{batt}}^{\mathrm{ref}})/\Delta t \quad (32)$$

$$\mathrm{P}_{\mathrm{bcar}}(t) = ((\mathrm{SOC}_{\mathrm{bcar}}(t + \Delta t) - \mathrm{SOC}_{\mathrm{bcar}}(t)).\mathrm{V}_{\mathrm{dc}}.\mathrm{C}_{\mathrm{bcar}}^{\mathrm{ref}})/\Delta t \quad (33)$$

Constraints (21) and (22) preserve the battery (BESS and electric car battery) and its life by operating it within a range of experimentally predetermined or manufacturer-required values. The state of charge of the main storage system battery (BESS) is maintained between 20% and 90% and that of the electric car battery between 20% and 80%. Outside these values, the battery can suffer serious problems (reduced efficiency, overvoltage, reduction of its total capacity...).

Constraints (23) and (24) represent the limit on the power variation, in absolute value, of P_{batt} and P_{bcar}.

Equations (25) and (26) represent the constraint on the variation of the state of charge between two sampling periods, which corresponds to the rate at which the battery (BESS or car battery) charges or discharges. It is assumed that the state of charge, during a sampling period Δt=10min, cannot vary by more than a rate of ±20% for the BESS and ±5% for the electric vehicle battery.

Equations (27) and (28) represent the constraints on the state of health of the batteries in order to use them optimally and efficiently.

Constraint (29) represents the limits related to the volume of the hydrogen tank (constraint on the hydrogen levels).

Constraint (30) represents the optimal operating range, with better efficiency, of the gas turbine [27].

The constraint (31) is on the power demand (excess or lack of energy) at which the supercapacitor starts to react instantly.

The constraint (30) is not considered as strict, i.e., the strategies which do not respect this limit, $\mathrm{P}_{\mathrm{gt}}(t) \geq \mathrm{P}_{\mathrm{gt}}^{\max}$ or $\mathrm{P}_{\mathrm{gt}}(t) \leq \mathrm{P}_{\mathrm{gt}}^{\min}$, are not deleted, but a penalty is

applied on the performance criterion if it is not verified (Equation (34)) :

$$CG(t) = C_{gt,Pen} \times (a_{gt} \times P_{gt}^2 + b_{gt} \times P_{gt} + c_{gt}) \times \Delta t \quad (34)$$

3.3 Priority Rules for the Use of System Components

For both strategies studied in this work, there are rules for using the different components of the system by priority. In case of overproduction ($P_{load}<P_{wt}+P_{pv}$), if the BESS is fully charged or if the charging power, P_{batt}, does not absorb this excess energy, the excess, $P_{wt}+P_{pv}-P_{load}-P_{batt}$, is stored as hydrogen energy according to the storage capacity of the tank, then and if the hydrogen tank is full, the excess, $P_{wt}+P_{pv}-P_{load}-P_{batt}-P_{elec}$, can be stored in the battery of the electric vehicle, if it is connected to the microgrid and that $SOC_{bcar} < SOC_{bcar}^{max}$. In case of underproduction ($P_{load}>P_{wt}+P_{pv}$), if the BESS is discharged or if the discharge power, P_{batt}, is not sufficient to cover the need, the energy shortage, $P_{wt}+P_{pv}-P_{load}-P_{batt}$, is covered by the fuel cell at the limit of the hydrogen storage capacity ($NH>NH_{min}$), then and if the hydrogen tank is empty, the lack of energy, $P_{wt}+P_{pv}-P_{load}-P_{batt}-P_{fc}$, can be covered by discharging the battery of the electric vehicle provided that the vehicle is connected to the microgrid and that $SOC_{bcar}>SOC_{bcar}^{min}$, then, if there is still a lack of energy, $P_{wt}+P_{pv}-P_{load}-P_{batt}-P_{fc}-P_{bcar}$, the gas turbine can be started to cover the energy need. The above-mentioned constraints must be respected.

4. Dynamic Programming - Energy Management Problem

The system is defined as a multi-step process. The system states are the discrete values of the battery state of charge (BESS) shifted by one step of δSOC_{batt}. Any path, between the two nodes i and j, that meets the constraint in equation (25) is a probable path for the algorithm as long as the battery state of charge values meet the constraint in equation (21). The initial state of charge ($SOC0_{batt}$) is given as the initial node. Similarly, the final state of charge ($SOCT_{batt}$), at the end of the day, is defined. All edges are oriented in one direction from t to t+Δt. Thus, the SOC change process is seen as a graph oriented in the forward direction. Therefore, Bellman algorithm is used to find the shortest path through the system and to minimize the cash flow value by finding the optimal SOC_{batt} transition sequence. [15].
Figure 5 illustrates the topology of the algorithm with all possible paths from the $SOC0_{batt}$ state, corresponds to node 0, to the final $SOCT_{batt}$ state, corresponds to node T. We define 8 different possible states at each sampling step that are shifted by δSOC_{batt} by 10%, between the minimum 20% and maximum 90% charge state.

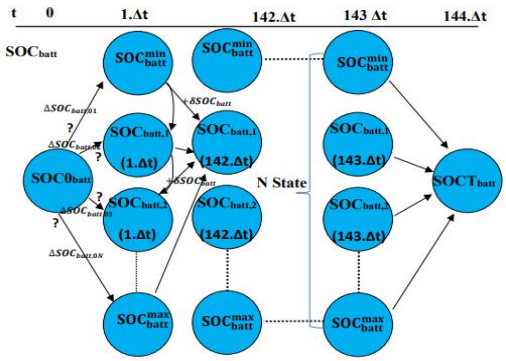

Fig. 5. Topology of the dynamic programming algorithm.

The problem is discretized in time steps "Δt =10 min". The number of states "N", representing sampled time values based on a sampling step (Δt) for the 24-hour period, according to the imposed bounds is 144 (Equation (35)):

$$N = \frac{SOC_{batt}^{max} - SOC_{batt}^{min}}{\delta SOC} = 144 \quad (35)$$

The arrows in Fig.5 connect the nodes of the system represent all possible trajectories. Each arrow corresponds to the change in battery state of charge $\Delta SOC_{batt}(x_i, x_j, t)$ between two nodes x_i and x_j. An arrow must always connect two nodes offset by Δt where xj is at time t while xi is at time t-Δt. The initial and final values of the nodes in the system are predetermined.

At each time step, the battery power's estimation is based on the ΔSOC_{batt} value (according to the constraints) [29]. The initial load state "$SOC0_{batt}$" is the only summit that has no predecessor. In order to compare policies of the same order, the final state "$SOCT_{batt}$" is imposed identical to the initial state. All arcs are oriented in the same direction from time "t" to time "t+Δt". This is a directed state graph, Fig.5, that has no circuits and that respects the conditions of application of the Bellman algorithm.

The BESS power (P_{batt}) is estimated at each stage of charge variation ΔSOC_{batt}. Then, the power of the gas turbine "P_{gt}", the power of the electrolyzer "P_{elec}", the power of the fuel cell "P_{fc}" and the power of the electric car battery P_{bcar}" are calculated following the P_{batt}, P_{load}, P_{wt} and P_{pv}, respecting the constraints and rules of operation by priority of each component. Finally, the CF corresponding is achieved, and it is the edge of the SOC graph.

Figure 6 shows the flowchart of the algorithm DP with the detailed calculation of the arc weights:

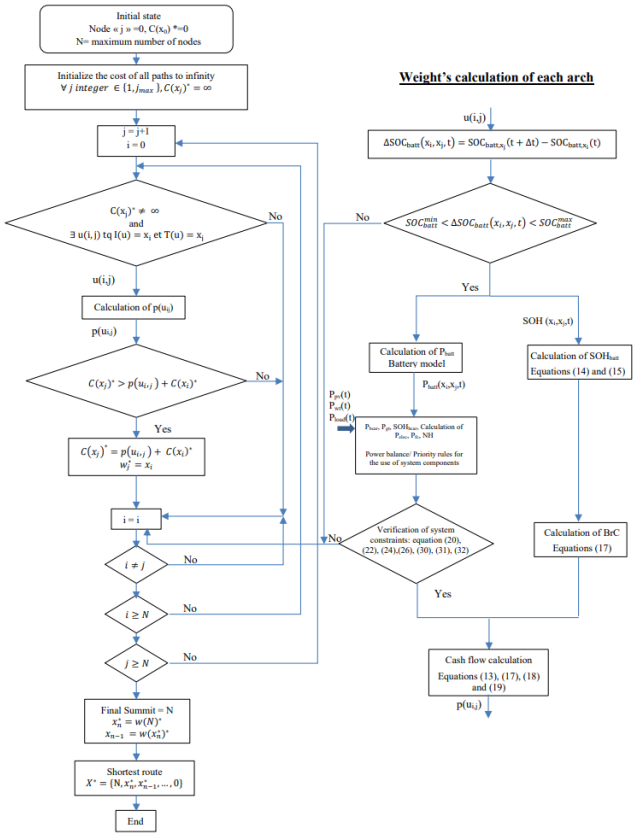

Fig. 6. The flowchart of the energy management strategy based on DP.

5. Rule-Based Method

In this section, a rule-based strategy, called restricted, will be proposed. It is called restricted because it does not consider the SOH of the batteries in the predefined rules. The operating mode is imposed according to the power value of the renewable resources and the consumption and based on human expertise and knowledge of the consumption and production profile [15].

The principle of the restricted management is based on the following three main rules:

- Photovoltaic and wind energy are used primarily to power the loads.
- In case of underproduction and the BESS is discharged or one of the constraints (23 & 25) is not verified anymore, then this energy need is provided first by the fuel cell at the limit of the hydrogen storage capacity and in case the fuel cell does not provide this shortage or that the level of stored hydrogen is at its highest level, the energy need is ensured by the battery of the electric vehicle, provided that the vehicle is connected to the micro-grid, then and if there is still a shortage of energy, the gas turbine can be started to cover the energy need.
- In case of overproduction and if the BESS is fully charged, the excess is stored as hydrogen energy according to the storage capacity of the tank, then and if the hydrogen tank is full, the excess can be stored in the battery of the electric vehicle, if it is connected to the microgrid.
- The BESS is recharged as soon as possible with the available renewable source (in case of overproduction).

The last rule is the most restrictive, ensuring that the BESS is loaded first in case of overproduction. Indeed, since no reliable information is known about the future, it is necessary to take advantage of every opportunity to charge the BESS and ensure that it has enough energy for the next unexpected discharge, in case of underproduction.

The synthesis of the proposed management method is summarized in the following flowchart:

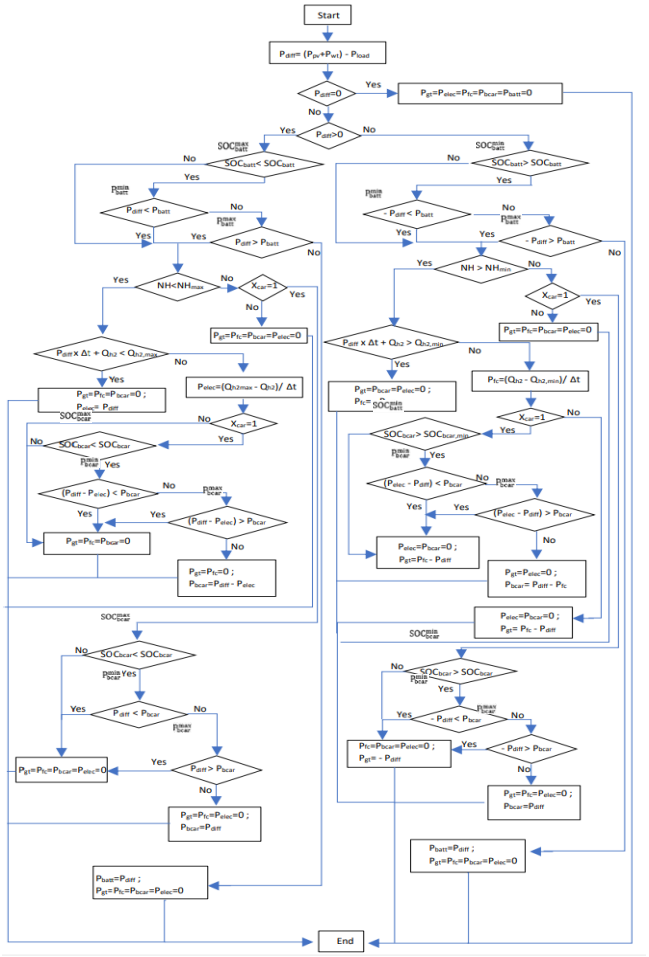

Fig. 7. The flowchart of the energy management strategy - Rule based method.

The system has been adapted to deterministic rule-based management using the "On/Off" strategy method.

6. Results And Discussion:

Table 1 represents the characteristics of the system as well as the simulation values of the parameters:

Table 1. The simulation parameter & characteristic of the system studied values

T	24h
ΔT	10 min
δSOC_{batt}	10%
$SOC0_{batt}$	50%
$SOCT_{batt}$	50
$SOC_{batt}^{max}, SOC_{batt}^{min}$	90%, 20%
$SOC_{bcar}^{max}, SOC_{car}^{max}$	80%, 40%
$\Delta SOC_{batt}^{max}, \Delta SOC_{bcar}^{max}$	20%
$\Delta SOC_{batt}^{min}, \Delta SOC_{bcar}^{min}$	10%, 0.1%
V_{dc}	48 V
SOH_{min}	70%
C_{batt}^{ref}	100 Ah
C_{bcar}^{ref}	500 Ah
$P_{batt}^{max}, P_{batt}^{min}$	5.76 KW, 2.88 kW
$P_{bcar}^{max}, P_{bcar}^{min}$	28.8 kW, 0.144 kW
NH_{max}	95%
NH_{min}	10%
NHO	65%
$P_{gt}^{max}, P_{gt}^{min}$	6 kW, 3.3 kW
$P_{gt,nom}$	6.66 kW
C_{fc}	0.12 €/kwh
C_{gt}	0,257 €/kwh
$C_{gt,Pen}$	2.57 €/kwh
C_{sc}	50 F
Q_{H2max}	10 kWh
Techno PV	Polycrystalline S.P
Techno Bat	Lithium-ion battery
BiC	140 (€)
Z	0.17×10-4
P_{pv}^{max}	9 kW
P_{wt}^{max}	6 kW

Figures 8 and 9 show the distribution curves obtained with the dynamic programming strategy and with the rule-based strategy:

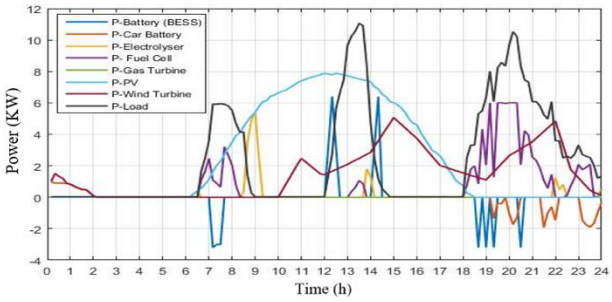

Fig. 8. Power flow of the system using DP method.

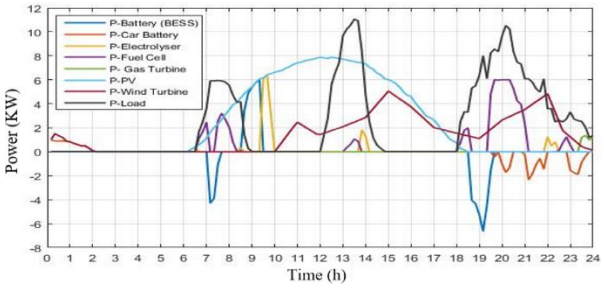

Fig. 9. Power flow of the system using rule-based method.

Energy management is better controlled with the dynamic programming method than with the rule-based method. With dynamic programming, a different battery charge/discharge strategy is used than with the rule-based management. Indeed, the strategy based on dynamic programming allows to manage the state of charge of the batteries in an optimal way, to discharge the batteries only when the production of the renewable sources is insufficient to cover the needs of the load and allows to minimize the use of the gas turbine and to decrease the cost by respecting all the mentioned constraints, a lower cash flow is expected with the management based on dynamic programming than with the method based on rules.

The figures above, 10 and 11, show the variation in battery SOC for the two methods used:

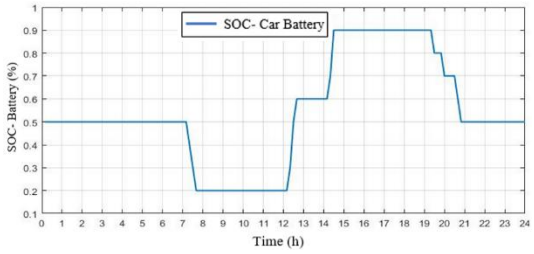

Fig. 10. SOC of the BESS using DP method.

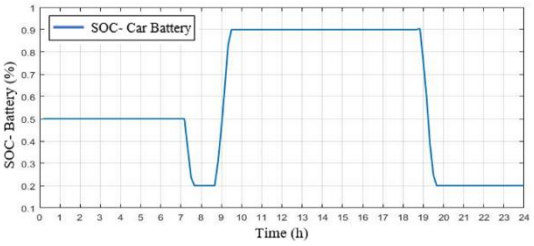

Fig. 11. SOC of the BESS using rule-based method.

With dynamic scheduling scheduling-based, the initial state of charge at t=0 ($SOC0_{batt}$=50%) is equal to the final state of charge at t=T ($SOCT_{batt}$=50%), which gives more flexibility to start the next day, but with the rule-based method, the final state of charge of the BESS is 20%, at its minimum level ($SOCT_{batt}=SOC_{batt}^{min}$).

The state of charge of the hydrogen tank, energy stored in the form of hydrogen, for the two proposed strategies, based on dynamic programming and rules, is presented in Fig.12 and Fig.13 respectively. with dynamic scheduling-based strategy, the level of energy stored in the tank at the end of the day is 3.3 kWh, so it does not reach its minimum value of 1 kWh, which gives more flexibility to start the next day. In contrast,

with the rule-based strategy, the reservoir is at its minimum level at the end of the day.

Knowing that, the tank initially contains 10 kWh of hydrogen equivalent energy at the beginning of the day.

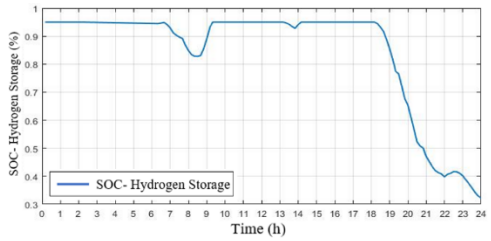

Fig. 12. SOC of the hydrogen storage tank using DP method.

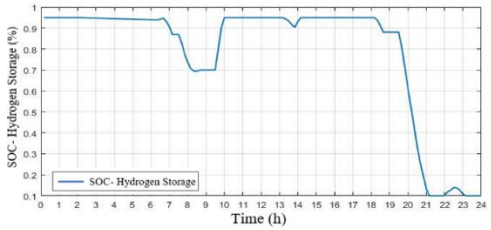

Fig. 13. SOC of Hydrogen storage using Rule-based method.

The following two figures (Fig.14 and Fig.15) illustrate the variation of the SOC of the electric car battery. With both methods (DP & rule-based strategies), the state of charge at the end of the usage periods is higher than the minimum state of charge value SOC_{bcar}^{min} (40%). In case of underproduction, the electric car batteries can be charged by the surplus energy after charging the BESS and the hydrogen tank (within the limits imposed by the state of charge of the car battery). In case of underproduction and the BESS is discharged as well as the hydrogen tank is at its low level, the batteries of the electric vehicle can be used (discharge), to avoid starting the gas turbine, in order to cover the energy need. The batteries of the electric vehicle are used (charge/discharge) only for the periods when the vehicle is connected to the microgrid.

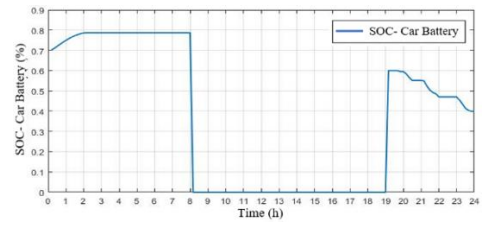

Fig. 14. SOC of the car battery using DP method.

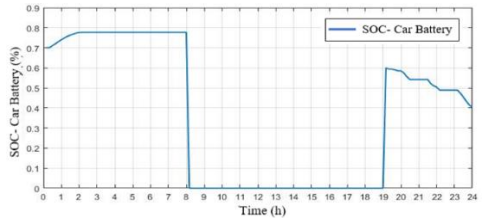

Fig. 15. SOC of the car battery using Rule-based method.

The following figures (Fig.16 & Fig.17) illustrate respectively the power of the supercapacitor and its state of charge. Supercapacitors are characterized by their instantaneous response time, compared to the other components of our studied system (BESS battery, gas turbine, fuel cell, electrolysis, car battery), in order to substitute the excess or lack of energy for a period of 10 seconds, time largely sufficient for our system components to respond. In our case, supercapacitors are used only if the excess or lack of energy exceeds a power of 0.5 kW, for each time step (within the limits imposed by the state of charge of the supercapacitors). The state of charge of the supercapacitor varies between 65% and 99% (charge/discharge) throughout the day.

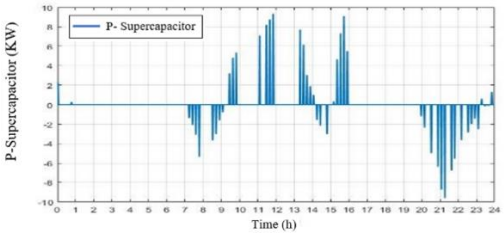

Fig. 16. Supercapacitor power variation.

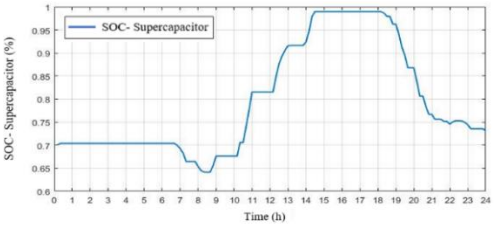

Fig. 17. SOC of the supercapacitor.

The final value of the objective function, using the two proposed strategies, is presented in Table 2.

Table 2. The final value of the objective function

	Rule-based method	Dynamic programming
Final Value (€)	**1.33**	**1.1**

The value of the cash flow, at the end of the day, with the dynamic programming-based method is lower than that found with the rule-based method. On the other hand, the computation time of the dynamic programming-based strategy is about 2.5 seconds, which is a little higher than that of the rule-based strategy (1 seconds).

The following two figures (Fig.18 & Fig.19) show the variation of the Cash Flow, for 24h, with the dynamic programming and rule-based strategy:

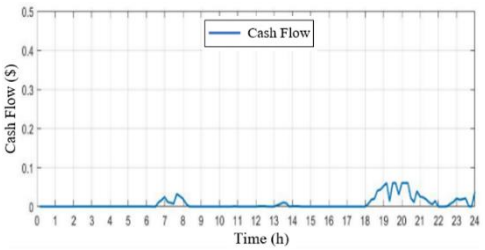

Fig. 18. Cash flow – DP method.

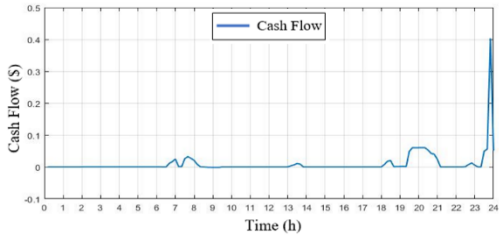

Fig. 19. Cash flow – Rule-based method.

7. Energy Management Strategies with correction

Some input data are difficult to predict with good reliability, mainly the weather conditions (irradiation and ambient temperature as well as wind speed), the consumption profile ("P_{load}") and the periods of connection of the electric vehicle to the microgrid.

The following figures, Fig.20 and Fig.21, show the power curves of the real-time photovoltaic & wind generation and the predicted generation curves.

- 50% error in PV power availability :

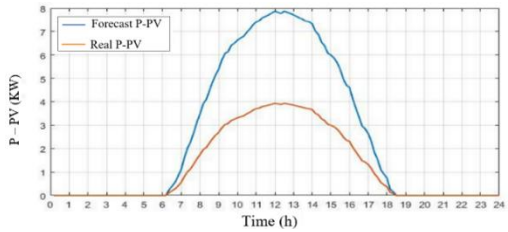

Fig. 20. The real PV production curve s the forecast curve.

- 10% error on the availability of wind energy :

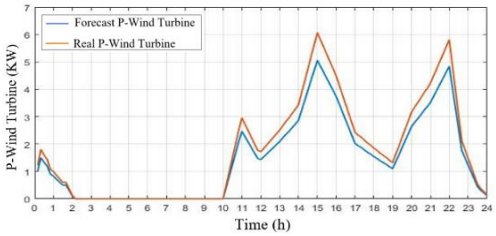

Fig. 21. The real wind power production curve Vs forecast curve.

The predicted connection periods of the electric car to the microgrid are different from those in real time. Between 12:30 and 13:30 of the day, the electric car connected to the microgrid unexpectedly. The forecasted load curve is considered to be identical to the real time curve.

Due to these prediction errors, disturbances, the proposed predictive strategies do not necessarily guarantee an optimal energy management, the photovoltaic and wind production is then no longer valued, and the system loses a large part of its interest. For this reason, we will develop correction algorithms, capable of modifying the predictive strategy according to the prediction errors (disturbance), to ensure the efficiency of the system.

7.1 Correction of the rule-based strategy

The principle of the rule-based strategy with correction is to apply predictive management strategy, discussed in section 5, as long as the constraints are respected and to modify it only in the presence of critical disturbances, so that the constraints are always verified. The approach is as follows:

- Application of the predictive strategy, based on rules, and calculation of the operation setpoints and power (P_{gt}, P_{fc}, P_{batt}, P_{bcar}, P_{elec}) of the various components of the system.
- If the disturbances are not critical and all constraints are verified, predictive control is maintained.
- If the disturbances are critical, one of the constraints is not verified, a new predictive command is imposed considering these disturbances so that all constraints are respected.
- Calculation of the new commands, which checks the different constraints according to the critical disturbances.

7.2 Dynamic programming strategy with correction

Bellman's algorithm is a graphical method of dynamic programming whose interest lies in the principle of optimality. A policy is optimal if, at a given period, whatever the previous decisions, the remaining decisions constitute an optimal policy with respect to the result of the previous decisions. Based on this optimality principle, we will readjust the strategy based on dynamic programming, proposed previously, according to the prediction errors and the different disturbances so that it is modified after each disturbance even for those which are not critical. This corresponds to the resolution of the global optimization problem at each perturbation.

The proposed correction principle is based on a reactive optimization which consists in reversing the direction of the shortest path problem in the weighted state graph from the final state to the initial state (reverse direction). We therefore construct the tree of optimal sub-policies to return to the initial state from the final state. This is possible because we work in finite horizon and we know the final state and the initial state, both imposed, as illustrated in the following figure:

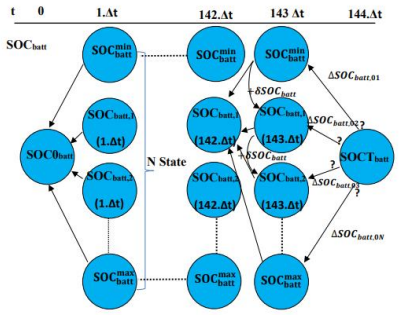

Fig. 22. Topology of the dynamic programming algorithm in reverse direction.

If we read the graph in Fig.22, in the reverse direction, the cost associated with each state corresponds to the costs of the optimal sub-policies that lead to the final state of imposed

load, the corresponding path passes through state "xj" at time t+Δt to the next state at xi at time t. The cost of the shortest path between vertex "xi" and the final vertex is given by the following equation (36):

$$C(xi)^* = \min_{yj}\left(P\left(u_{xi,yj}\right) + C(yj)^*\right) \quad (36)$$

With

C(yi)*: The cost of the shortest path between vertex "j" and the final vertex.

Uxi,xj: Arc between vertex " yj " and the previous vertex "xi "

The weight of the arc "P (Uxi,xj)", between two states xi and xj, depends only on these two nodes and not on previous decisions.

With this strategy, after any prediction error or disturbance, at a given time step, the weights of the arcs between the different nodes are recalculated for the remaining vertices. A new optimal policy, consisting of the remaining decisions, and the operating set points of each component of the system are recalculated considering the new arc weights.

7.3 Results and Discussion

The following two figures (Fig.23 & Fig.24) show the difference between the power curve representing the energy need/excess, P_{load}-P_{pv}-P_{wt}, and the curve representing the power of the various other elements constituting our system, P_{gt}+P_{fc}-P_{batt}-P_{bcar}-P_{elec}, for the two proposed strategies without correction based on dynamic programming and the one based on rules respectively. The operating set points of each component are predefined based on the forecasted input data, without correction, the fact that can directly impact the quality of energy management after each disturbance, e.g. in case of overproduction in real time, the surplus energy may not be stored by the batteries or in the hydrogen tank (loss of energy) and in the case of underproduction, the consumption of the load may not be covered, which can generate an imbalance between production and consumption. For example, between 12:30 and 13:30, although the production of renewable energies does not cover the demand of the load, the gas turbine as well as the fuel cell and the batteries of the electric vehicle are not used to cover this lack of energy, since the control setpoints of the various components of the system are calculated without taking into account this unexpected disruption.

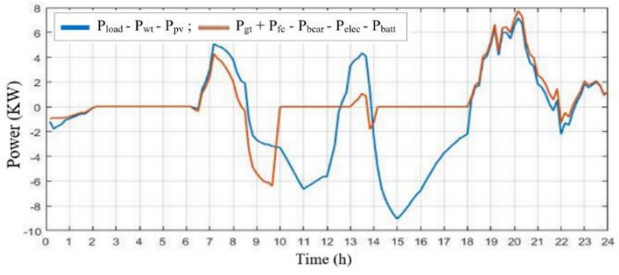

Fig. 23. Energy requirement/surplus Vs Energy supplied by BESS and auxiliary sources - DP without correction.

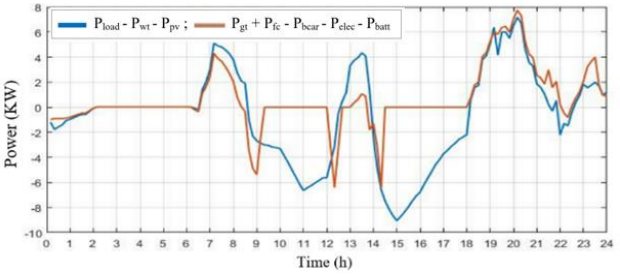

Fig. 24. Energy requirement/surplus Vs Energy supplied by BESS and auxiliary sources – Rule-based method without correction.

Figures 25 and 26 show the power distribution curves obtained with the strategies, with correction, based on dynamic programming and rules-based method.

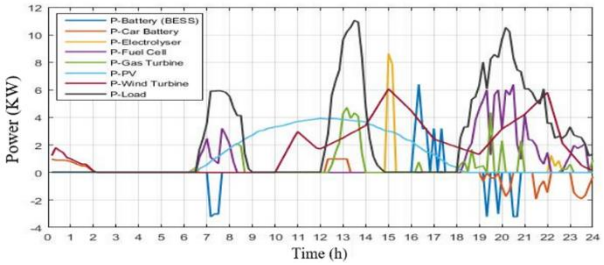

Fig. 25. Power flow of the system using DP method.

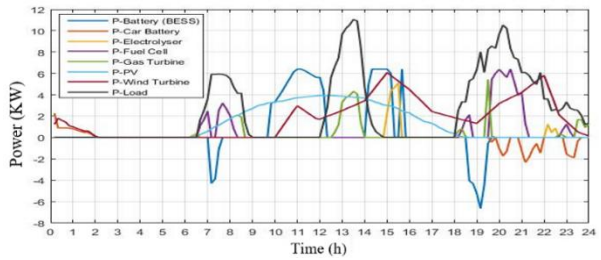

Fig. 26. Power flow of the system using Rule-based method.

Energy management, with correction, is controlled more optimally and efficiently with the dynamic scheduling method than with the rule-based method. With the dynamic programming and in case of disturbance (real-time data different from the predicted ones), the strategy is corrected and modified for the rest of the day so that the energy is managed in an optimal way by optimizing the use of the BESS and the hydrogen storage system, readjusting and correcting the control set points of the different elements of the system after each disturbance, whether critical or not, and minimizing the use of the gas turbine, making better use of the storage system of the electric car to feed the load in case of underproduction, which contributes to a good management with a minimal operating cost. On the other hand, the rule-based strategy is modified only during the period when there are disturbances and not during the rest of the day or with non-critical disturbances, which can impact the efficiency of using the different system components in an optimal way with higher operating costs.

The following two figures (Fig.27 and Fig.28) show the difference between the power curve representing the energy need/excess, and the curve representing the power of the

various other elements constituting our system, for the two proposed strategies with correction. The operating control setpoints for each element are calculated based on the predicted input data, but after each disturbance, the control setpoints are recalculated and corrected taking these disturbances into account.

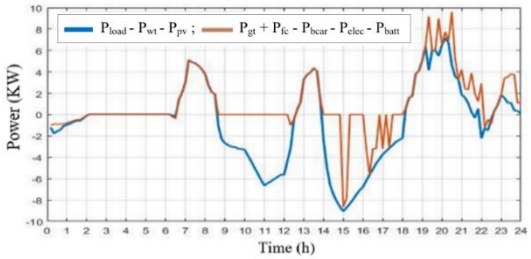

Fig. 27. Energy requirement/surplus Vs Energy supplied by BESS and auxiliary sources - DP with correction.

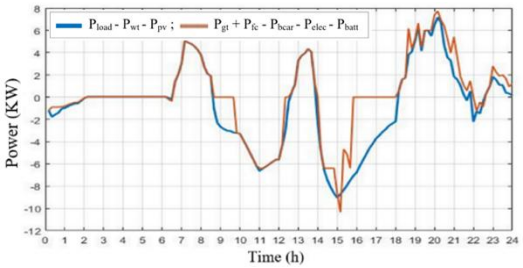

Fig. 28. Energy requirement/surplus Vs Energy supplied by BESS and auxiliary sources – Rule-based method.

The state of charge of the hydrogen tank, for the two proposed strategies with correction, based on dynamic programming and rules, is presented in Fig.29 and Fig.30 respectively. with dynamic scheduling-based strategy, the level of energy stored in the tank at the end of the day is 3 kWh, so it does not reach its minimum value of 1 kWh, which gives more flexibility to start the next day. In contrast, for the rule-based strategy, the reservoir is at its minimum level at the end of the day.

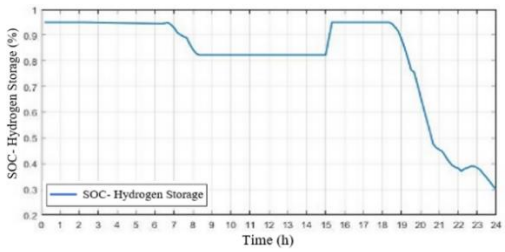

Fig. 29. SOC of hydrogen storage tank using DP method.

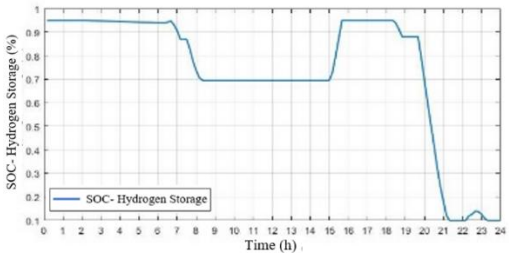

Fig. 30. SOC of hydrogen storage tank using Rule-based method.

The figures above (Fig.31 & Fig.32) show the variation in battery SOC (BESS) for the two methods used:

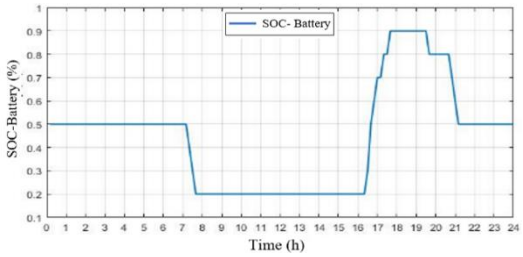

Fig. 31. SOC of the BESS using DP method.

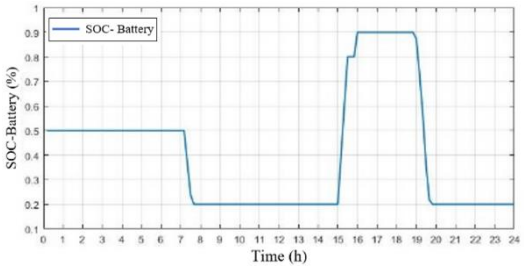

Fig. 32. SOC of the BESS using Rule-based method.

With dynamic scheduling scheduling-based, the initial state of charge at t=0 ($SOC0_{batt}$=50%) is equal to the final state of charge at t=T ($SOCT_{batt}$=50%), which gives more flexibility to start the next day, but with the rule-based method, the final state of charge of the BESS is 20%, at its minimum level ($SOCT_{batt}=SOC_{batt}^{min}$).

The following two figures (Fig.33 and Fig.34) illustrate the variation of the SOC of the electric car battery. With both methods with correction (DP & rule-based strategies):

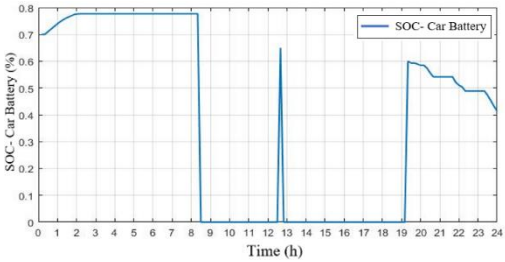

Fig. 33. SOC of the car battery using DP method.

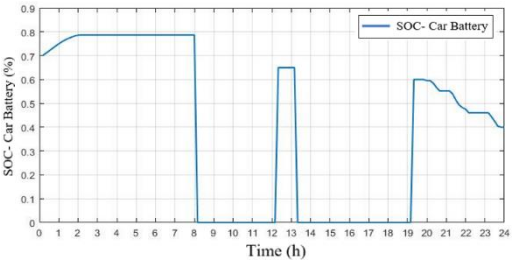

Fig. 34. SOC of the car battery using Rule-based method.

Between 12:30 and 13:30, the vehicle connected to the micro grid unexpectedly (disturbance). With the dynamic programming-based correction strategy, the batteries of the electric vehicle were used, within the limits imposed by the state of charge of the car battery, during this period to cover

the energy requirement, which allowed us to avoid the use of the fuel cell and gas turbine as well as to reduce the operating cost of the system. With the rule-based method, the batteries of the electric vehicle were not used to cover this energy shortage, since the control setpoints of the different components of the system are calculated without considering this disturbance.

The following two figures (Fig.35 & Fig.36) show the variation of the Cash Flow for the two strategies used:

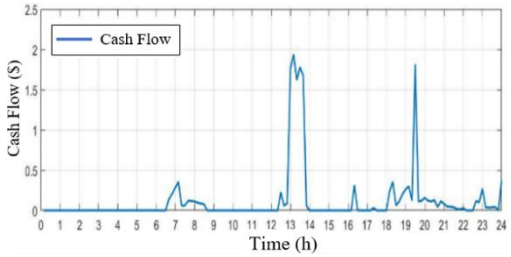

Fig. 35. Cash flow – DP method.

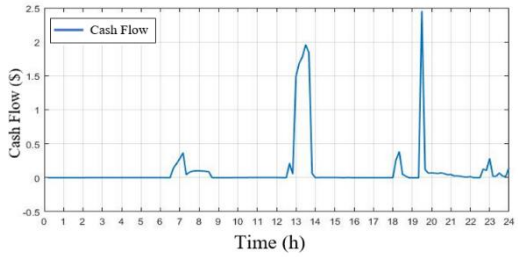

Fig. 36. Cash flow – Rule-based method.

The final value of the objective function, using the two proposed strategies, is presented in Table 3.

Table 3. The final value of the objective function

	Rule-based method	Dynamic programming
Final Value (€)	**16.94**	**14.82**

The value of the cash flow, at the end of the day, with the dynamic programming-based method is lower than that found with the rule-based method. On the other hand, the computation time of the dynamic programming-based strategy is about 4 s seconds, which is a little higher than that of the rule-based strategy (1.8 second).

8. CONCLUSION:

This work proposes a new centralized control for real-time and predictive energy management for an isolated microgrid, complicated hybrid system composed of several storage and generation elements, which has not been studied before , mainly composed of a photovoltaic generator, a wind turbine, a gas turbine, a battery, a supercapacitor, a load, an electric vehicle, and a hydrogen energy storage system consisting of a fuel cell, an electrolyzer, and a hydrogen tank. The central controller was developed using the Bellman-Ford algorithm, based on dynamic programming, to find the minimum cash flow with an optimal management of the sources, while respecting the constraints of the system. The effectiveness of this proposed strategy, based on dynamic programming, has been demonstrated and proven by the different simulations and results found previously and validated by comparing the results with those of the rule-based management strategy. However, it turns out that some input data are difficult to predict with good reliability, namely the weather conditions (irradiation and ambient temperature as well as wind speed), the consumption profile and the periods of connection of the electric vehicle to the microgrid. Given these prediction errors, the proposed strategies, without correction, do not necessarily guarantee an optimal and efficient energy management, the PV and wind energies are then no longer valued, and the system loses a large part of its interest. For this reason, correction algorithms have been developed, capable of modifying the predictive strategy according to the prediction errors (disturbance), in order to guarantee a good and efficient energy management. The strategy is thus modified for each disturbance, even for those which are not critical.

Future work will include new strategies for optimal energy management in real time by also integrating the forecast errors on the consumption profile, that have not been addressed in this work and that will allow to get closer to the reality in operation in the implementation of the optimized approach.

References

[1] M. Urbina, and Z. Li, "A fuzzy optimization approach to PV/battery scheduling with uncertainty in PV generation," in Proc. 38th North American IEEE Power Symp. (NAPS 2006), Carbondale, IL, 2006, pp.561–566

[2] A. Chaouachi, R. M. Kamel, R. Andoulsi, and K. Nagasaka, "Multiobjective intelligent energy management for a microgrid", IEEE Trans. Ind. Electron., vol. 60, no. 4, pp. 1688–1699, Apr. 2013

[3] P. García, J. P. Torreglosa, L. M. Fernández, and F. Jurado, "Optimal energy management system for stand-alone wind turbine/ photovoltaic/hydrogen/battery hybrid system with supervisory control based on fuzzy logic," Int. J. Hydrogen Energy, vol. 38, no. 33

[4] B. Lu, and M. Shahidehpour, "Short term scheduling of battery in a grid connected PV/battery system," IEEE Trans. Power Syst., vol. 20, no. 2, pp. 1053–1061, May 2005

[5] M. Koot, J. T. B. A. Kessels, B. de Jager, W. P. M. H. Heemels, P. P. J. Van Den Bosch, and M. Steinbuch, "Energy management strategies for vehicular electric power systems," IEEE Trans. Veh. Technol., vol. 54, no. 3, pp. 771–782, May 2005

[6] E. Sortomme, and M. A. EI-Sharkawi, "Optimal power flow for system of microgrids with controllable loads and battery storage," IEEE PES Power System Conf. and Exposition, pp. 1-5, 2009

[7] B. Ramachandran, Sanjeev K. Srivastava, Chris S. Edrington, and David A. Cartes, "An intelligent auction scheme for smart grid market using a hybrid immune algorithm", IEEE Trans. Industrial Electronics, vol. 58, No. 10, October 2011

[8] S. A. Pourmousavi, M. H. Nehrir, C. M. Colson, and C. Wang, "Realtime energy management of a stand-alone hybrid wind-microturbine energy system using particle swarm optimization," IEEE Trans. Sustain. Energy, vol. 1, no. 3, pp. 193–201, Oct. 2010

[9] S. Leonori , A. Martino, F. M. F. Mascioli, and Antonello Rizzi, "Microgrid Energy Management Systems Design by Computational Intelligence Techniques", Applied Energy 2020, 277, 115524

[10] L. Xu, and D. Chen, "Control and Operation of a DC Microgrid with Variable Generation and Energy Storage", IEEE Transactions on Power Delivery, Vol.26, Issue 4, Oct 2011

[11] S. Kotra, and M. K. Mishra, "Energy management of hybrid microgrid with hybrid energy storage system", 2015 International Conference on Renewable Energy Research and Applications, pp.856-860, November 2015

[12] W. Yeting, D. Yuxing, Z. Xiwei, W. Ye, and X. Bin, "Application of island microgrid based on hybrid batteries storage", 2014 International Conference on Renewable Energy Research and Application, pp.262-267, October 2014

[13] A. Tani, M.B. Camara, and B. Dakyo, "Energy management in the decentralized generation systems based on renewable energy sources", International Conference on Renewable Energy Research and Applications, 2012

[14] M. Elkazaz, M. Sumner, S. Pholboon, and D. Thomas, "Microgrid Energy Management Using a Two Stage Rolling Horizon Technique for Controlling an Energy Storage System", 2018 7th International Conference on Renewable Energy Research and Applications, pp.324-329, october 2018

[15] Y. Riffonneau, S. Bacha, F. Barruel, and S. Ploix, "Optimal Power Flow Management for Grid Connected PV Systems With Batteries", IEEE Transactions on Sustainable Energy, pp.309-320, Vol. 2, No. 3, july 2011

[16] C. Chen, S. Duan, T. Cai, B. Liu, and G. Hu, "Smart energy management system for optimal microgrid economic operation," IET Renew. Power Gener., vol. 5, Iss. 3, pp.258-267, 2011

[17] B. Zhao, X. Zhang, P. Li, K. Wang, M. Xue, and C. Wang, " Optimal sizing, operating strategy and operational experience of a standalone microgrid on Dongfushan Island", Applied Energy, 113: 1656-1666, January 2014.

[18] A. Aktas, K. Erhan, S. Özdemir, and E. Özdemir, "Dynamic energy management for photovoltaic power system including hybrid energy storage in smart grid applications", Energy, vol. 162, pp. 72_82, Nov. 2018.

[19] A. Borghetti, C. D'Ambrosio, A. Lodi, and S. Martello, "An MILP approach for short-term hydro scheduling and unit commitment with head-dependent reservoir", IEEE Trans. Power Syst., vol. 23, no. 3, pp. 1115–1124, Aug. 2008

[20] T.T. Ha Pham, F. Wurtz, and S. Bacha, "Optimal operation of a PV based multisource system and energy management for household application", IEEE International Conference on Industrial Technology, pp. 1-5. doi : 10.1109/ICIT.2009.4939701

[21] A. Saidi, A. Harrouz, I. Colak, K. Kayisli, and R. Bayindir, " Performance Enhancement of Hybrid Solar PV-Wind System Based on Fuzzy Power Management Strategy: A Case Study", 7th International Conference on Smart Grid, pp. 126-131, December 2019.

[22] S. Chakraborty , M. D. Weiss, and M. G. Simoes, "Distributed intelligent energy management system for a Single-Phase High-Frequency AC microgrid," IEEE Transactions on Industrial Electronics, vol.54, pp.97-109, 2007

[23] C.Wang, and M. H. Nehrir, "Power management of a stand-alone wind/photovoltaic/fuel cell energy system," IEEE Trans. Energy Convers.,vol. 23, no. 3, pp. 957–967, Sep. 2008

[24] C. Darras, S. Sailler, C. Thibault, M. Muselli, P. Poggi, J.C Hoguet, S. Melsco, E. Pinton,S. Grehant, F. Gailly, C. Turpin, S. Astier, and G. Fontès, "Sizing of photovoltaic system coupled with hydrogen/oxygen storage based on the ORIENTE model," InternationalJournal ofHydrogen Energy, Vol. 35, N°8, pp. 3322-3332, 2010

[25] Yi-Hwa Liu, and Jen-Hao Teng, "Design and Implementation of a Fully-digital Lithium-Ion Battery Charger", TENCON 2006 IEEE Region 10 Conference, November 2006

[26] S.M. Mousavi, S.H. Fathi, and G.H. Riahy, "Energy management of wind/PV and battery hybrid system with consideration of memory effect in battery", International Conference on Clean Electrical Power, pp.630-633, June 2009

[27] H. Kanchev, D. Lu, B. Francois, and V. Lazarov, "Smart monitoring of a microgrid including gas turbines and a dispatched PV-based active generator for energy management and emissions reduction", IEEE PES Innovative Smart Grid Technologies Conference Europe, October 2010

[28] Gangui Yan, Ke Feng, and Junhui Li, "Optimal Control of Combined Wind and Hydrogen System Based on Genetic Algorithm," 2016 International Conference on Smart City and Systems Engineering (ICSCSE). IEEE, 2016

[29] M. H. Laraki, B. Brahmi, and C. Z. ElBayeh, "Energy management system for a Stand-alone Wind/ Diesel/ BESS/ Fuel-cell Using Dynamic Programming 2021," 18th International Multi-Conference on Systems, Signals & Devices (SSD'21)